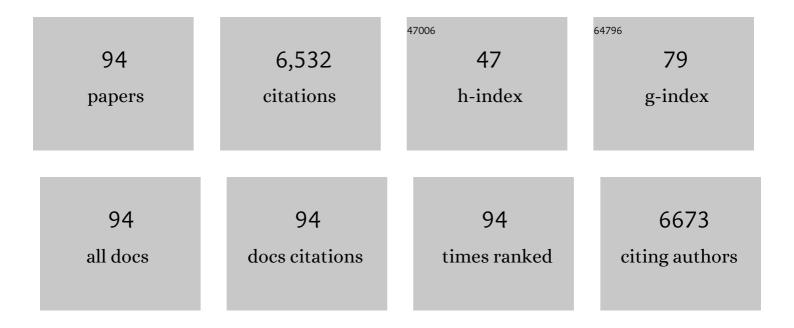
Xi-Tian Zhang

List of Publications by Year in descending order

Source: https://exaly.com/author-pdf/1501497/publications.pdf Version: 2024-02-01



#	Article	IF	CITATIONS
1	Mitigating side reaction for high capacity retention in lithium-sulfur batteries. Chinese Chemical Letters, 2022, 33, 457-461.	9.0	22
2	Tailoring the Spatial Distribution and Content of Inorganic Nitrides in Solid–Electrolyte Interphases for the Stable Li Anode in Li–S Batteries. Energy and Environmental Materials, 2022, 5, 1180-1188.	12.8	26
3	Regulation of impedance matching feature and electronic structure of nitrogen-doped carbon nanotubes for high-performance electromagnetic wave absorption. Journal of Materials Science and Technology, 2022, 108, 1-9.	10.7	5
4	V ₂ CT _{<i>X</i>} catalyzes polysulfide conversion to enhance the redox kinetics of Li–S batteries. Dalton Transactions, 2022, 51, 2560-2566.	3.3	6
5	Rational design of adsorption-catalysis functional separator for highly efficient Li-S batteries. Journal of Alloys and Compounds, 2022, 900, 163414.	5.5	2
6	Imbedding Li2CO3 in Li-nafion film to protect Li anode from unexpected dendrites growth. Journal of Alloys and Compounds, 2022, 900, 163444.	5.5	8
7	Photothermal-effect-promoted interfacial OH ^{â^'} filling and the conversion of carrier type in (Co _{1â^'<i>x</i>} Ni _{<i>x</i>}) ₃ C during water oxidation. Journal of Materials Chemistry A, 2022, 10, 8258-8267.	10.3	6
8	Computational screening of functionalized MXenes to catalyze the solid and non-solid conversion reactions in cathodes of lithium–sulfur batteries. Physical Chemistry Chemical Physics, 2022, 24, 8913-8922.	2.8	4
9	Shielding polysulfides enabled by a biomimetic artificial protective layer in lithium-sulfur batteries. Journal of Colloid and Interface Science, 2022, 625, 119-127.	9.4	4
10	Synergistic effect of cocatalytic NiSe ₂ on stable 1T-MoS ₂ for hydrogen evolution. RSC Advances, 2021, 11, 6842-6849.	3.6	7
11	Nb2CT MXene: High capacity and ultra-long cycle capability for lithium-ion battery by regulation of functional groups. Journal of Energy Chemistry, 2021, 53, 387-395.	12.9	61
12	A strategy to achieve high loading and high energy density Li-S batteries. Journal of Energy Chemistry, 2021, 53, 340-346.	12.9	35
13	An effective strategy for shielding polysulfides and regulating lithium deposition in lithium–sulfur batteries. Journal of Power Sources, 2021, 489, 229500.	7.8	14
14	Electrolyte Structure of Lithium Polysulfides with Antiâ€Reductive Solvent Shells for Practical Lithium–Sulfur Batteries. Angewandte Chemie - International Edition, 2021, 60, 15503-15509.	13.8	108
15	Electrolyte Structure of Lithium Polysulfides with Antiâ€Reductive Solvent Shells for Practical Lithium–Sulfur Batteries. Angewandte Chemie, 2021, 133, 15631-15637.	2.0	8
16	Partially contacted NixSy@N, S-codoped carbon yolk-shelled structures for efficient microwave absorption. Carbon, 2021, 182, 276-286.	10.3	47
17	Achieving dendrite-free lithium deposition on the anode of Lithium–Sulfur battery by LiF-rich regulation layer. Electrochimica Acta, 2021, 393, 138981.	5.2	16
18	One-step synthesis Nb2CT MXene with excellent lithium-ion storage capacity. Journal of Alloys and Compounds, 2021, 889, 161542.	5.5	14

#	Article	IF	CITATIONS
19	Promoting effect of MXenes on 1T/2H–MoSe ₂ for hydrogen evolution. CrystEngComm, 2021, 23, 4752-4759.	2.6	13
20	Tuning Dielectric Loss of SiO2@CNTs for Electromagnetic Wave Absorption. Nanomaterials, 2021, 11, 2636.	4.1	8
21	A Cobalt(II) Polymer Constructed by N,N '-Bis(3-Pyridinecarboxamide)-1,4-Benzene: Synthesis and Structural Characterization. Crystallography Reports, 2021, 66, 1286-1289.	0.6	2
22	Progress of Twoâ€Dimensional Ti ₃ C ₂ T _{<i>x</i>} in Supercapacitors. ChemSusChem, 2020, 13, 1296-1329.	6.8	45
23	Three-dimensional architectures assembled with branched metal nanoparticle-encapsulated nitrogen-doped carbon nanotube arrays for absorption of electromagnetic wave. Journal of Alloys and Compounds, 2020, 821, 153267.	5.5	14
24	N-doped reduced graphene oxide aerogels containing pod-like N-doped carbon nanotubes and FeNi nanoparticles for electromagnetic wave absorption. Carbon, 2020, 159, 357-365.	10.3	185
25	First-principles study of high performance lithium/sodium storage of Ti ₃ C ₂ T ₂ nanosheets as electrode materials*. Chinese Physics B, 2020, 29, 016802.	1.4	8
26	3D Ti3C2Tx aerogel-modified separators for high-performance Li–S batteries. Journal of Alloys and Compounds, 2020, 816, 153155.	5.5	15
27	Molybdenum-doped CuO nanosheets on Ni foams with extraordinary specific capacitance for advanced hybrid supercapacitors. Journal of Materials Science, 2020, 55, 2492-2502.	3.7	74
28	Effect of Ti3C2Tx–PEDOT:PSS modified-separators on the electrochemical performance of Li–S batteries. RSC Advances, 2020, 10, 40276-40283.	3.6	5
29	Direct observation of chemical origins in crystalline (Ni _x Co _{1â^x}) ₂ B oxygen evolution electrocatalysts. Catalysis Science and Technology, 2020, 10, 2165-2172.	4.1	10
30	Additive-free porous assemblies of Ti3C2T by freeze-drying for high performance supercapacitors. Chinese Chemical Letters, 2020, 31, 1034-1038.	9.0	10
31	A safe etching route to synthesize highly crystalline Nb2CTx MXene for high performance asymmetric supercapacitor applications. Electrochimica Acta, 2020, 337, 135803.	5.2	99
32	General strategy for fabrication of N-doped carbon nanotube/reduced graphene oxide aerogels for dissipation and conversion of electromagnetic energy. Journal of Materials Chemistry C, 2020, 8, 7847-7857.	5.5	51
33	Novel Li _x SiS _y /Nafion as an artificial SEI film to enable dendrite-free Li metal anodes and high stability Li–S batteries. Journal of Materials Chemistry A, 2020, 8, 8979-8988.	10.3	72
34	Flexible Ti ₃ C ₂ T _x /PEDOT:PSS films with outstanding volumetric capacitance for asymmetric supercapacitors. Dalton Transactions, 2019, 48, 1747-1756.	3.3	119
35	Metal organic framework-derived three-dimensional graphene-supported nitrogen-doped carbon nanotube spheres for electromagnetic wave absorption with ultralow filler mass loading. Carbon, 2019, 155, 233-242.	10.3	109
36	One-step synthesis of few-layer niobium carbide MXene as a promising anode material for high-rate lithium ion batteries. Dalton Transactions, 2019, 48, 14433-14439.	3.3	45

#	Article	IF	CITATIONS
37	Three dimensional graphene-supported nitrogen-doped carbon nanotube architectures for attenuation of electromagnetic energy. Journal of Materials Chemistry C, 2019, 7, 11868-11878.	5.5	50
38	Large-Scale Synthesis of Three-Dimensional Reduced Graphene Oxide/Nitrogen-Doped Carbon Nanotube Heteronanostructures as Highly Efficient Electromagnetic Wave Absorbing Materials. ACS Applied Materials & Interfaces, 2019, 11, 39100-39108.	8.0	110
39	Ultrasmall FeNi ₃ N particles with an exposed active (110) surface anchored on nitrogen-doped graphene for multifunctional electrocatalysts. Journal of Materials Chemistry A, 2019, 7, 1083-1091.	10.3	89
40	Understanding the Different Diffusion Mechanisms of Hydrated Protons and Potassium Ions in Titanium Carbide MXene. ACS Applied Materials & Interfaces, 2019, 11, 7087-7095.	8.0	36
41	The integration of Mo ₂ C-embedded nitrogen-doped carbon with Co encapsulated in nitrogen-doped graphene layers derived from metalâ€ ⁴ organic-frameworks as a multi-functional electrocatalyst. Nanoscale, 2019, 11, 12563-12572.	5.6	39
42	Current-density dependence of Li ₂ S/Li ₂ S ₂ growth in lithium–sulfur batteries. Energy and Environmental Science, 2019, 12, 2976-2982.	30.8	102
43	The surface engineering of cobalt carbide spheres throughÂN, B co-doping achieved by room-temperature <i>in situ</i> anchoring effects for active and durable multifunctional electrocatalysts. Journal of Materials Chemistry A, 2019, 7, 14904-14915.	10.3	88
44	Dual effects of the carbon fibers/Ti3C2Tx interlayer on retarding shuttle of polysulfides for stable Lithium-Sulfur batteries. Electrochimica Acta, 2019, 312, 149-156.	5.2	50
45	Free-standing MXene film modified by amorphous FeOOH quantum dots for high-performance asymmetric supercapacitor. Electrochimica Acta, 2019, 308, 1-8.	5.2	72
46	Towards full demonstration of high areal loading sulfur cathode in lithium–sulfur batteries. Journal of Energy Chemistry, 2019, 39, 17-22.	12.9	87
47	In situ polymerized Ti3C2Tx/PDA electrode with superior areal capacitance for supercapacitors. Journal of Alloys and Compounds, 2019, 778, 858-865.	5.5	63
48	One-pot synthesis of SL-MoS2/C/Ti3C2Tx@C hierarchical superstructures for ultralong cycle-life Li-ion batteries. Electrochimica Acta, 2019, 295, 286-293.	5.2	8
49	Three-Dimensional Hierarchical MoS ₂ Nanosheets/Ultralong N-Doped Carbon Nanotubes as High-Performance Electromagnetic Wave Absorbing Material. ACS Applied Materials & Interfaces, 2018, 10, 14108-14115.	8.0	170
50	Self-supported NiMo-based nanowire arrays as bifunctional electrocatalysts for full water splitting. Journal of Materials Chemistry A, 2018, 6, 8479-8487.	10.3	134
51	Self-supported cobalt nitride porous nanowire arrays as bifunctional electrocatalyst for overall water splitting. Electrochimica Acta, 2018, 273, 229-238.	5.2	98
52	Role of the H-containing groups on the structural dynamics of Ti 3 C 2 T x MXene. Physica B: Condensed Matter, 2018, 537, 155-161.	2.7	17
53	An ultra-small NiFe ₂ O ₄ hollow particle/graphene hybrid: fabrication and electromagnetic wave absorption property. Nanoscale, 2018, 10, 2697-2703.	5.6	184
54	Synthesis and characterization of three-dimensional MoS2@carbon fibers hierarchical architecture with high capacity and high mass loading for Li-ion batteries. Journal of Colloid and Interface Science, 2018, 510, 327-333.	9.4	27

#	Article	IF	CITATIONS
55	Self-assembled Ti3C2Tx/SCNT composite electrode with improved electrochemical performance for supercapacitor. Journal of Colloid and Interface Science, 2018, 511, 128-134.	9.4	107
56	First-principle study of the Nb+1C T2 systems as electrode materials for supercapacitors. Computational Materials Science, 2018, 143, 225-231.	3.0	26
57	Nickel Nanoparticle Encapsulated in Few-Layer Nitrogen-Doped Graphene Supported by Nitrogen-Doped Graphite Sheets as a High-Performance Electromagnetic Wave Absorbing Material. ACS Applied Materials & Interfaces, 2018, 10, 1399-1407.	8.0	155
58	Growth of CoFe ₂ O ₄ hollow nanoparticles on graphene sheets for high-performance electromagnetic wave absorbers. Journal of Materials Chemistry C, 2018, 6, 12781-12787.	5.5	82
59	3D Ti ₃ C ₂ T _x aerogels with enhanced surface area for high performance supercapacitors. Nanoscale, 2018, 10, 20828-20835.	5.6	105
60	Feâ€Niâ€Mo Nitride Porous Nanotubes for Full Water Splitting and Znâ€Air Batteries. Advanced Energy Materials, 2018, 8, 1802327.	19.5	227
61	Hierarchical Hollow Spheres Assembled with Ultrathin CoMn Double Hydroxide Nanosheets as Trifunctional Electrocatalyst for Overall Water Splitting and Zn Air Battery. ACS Sustainable Chemistry and Engineering, 2018, 6, 14641-14651.	6.7	51
62	Enhanced electromagnetic wave absorption induced by void spaces in hollow nanoparticles. Nanoscale, 2018, 10, 18742-18748.	5.6	88
63	Nitrogen-doped carbon nanosheets containing Fe3C nanoparticles encapsulated in nitrogen-doped graphene shells for high-performance electromagnetic wave absorbing materials. Carbon, 2018, 140, 368-376.	10.3	93
64	Ti3C2Tx-foam as free-standing electrode for supercapacitor with improved electrochemical performance. Ceramics International, 2018, 44, 13901-13907.	4.8	31
65	Ag-Nanoparticle-Decorated 2D Titanium Carbide (MXene) with Superior Electrochemical Performance for Supercapacitors. ACS Sustainable Chemistry and Engineering, 2018, 6, 7442-7450.	6.7	120
66	Hollow N-Doped Carbon Polyhedron Containing CoNi Alloy Nanoparticles Embedded within Few-Layer N-Doped Graphene as High-Performance Electromagnetic Wave Absorbing Material. ACS Applied Materials & Interfaces, 2018, 10, 24920-24929.	8.0	224
67	Rationally designing S/Ti ₃ C ₂ T _x as a cathode material with an interlayer for high-rate and long-cycle lithium–sulfur batteries. Nanoscale, 2018, 10, 16935-16942.	5.6	50
68	A facile and green template-engaged synthesis of PbSe nanotubes with the assistance of Vc. CrystEngComm, 2018, 20, 5570-5575.	2.6	4
69	Free-standing Ti ₃ C ₂ T _x electrode with ultrahigh volumetric capacitance. RSC Advances, 2017, 7, 11998-12005.	3.6	98
70	Highly Stable Threeâ€Dimensional Porous Nickelâ€ŀron Nitride Nanosheets for Full Water Splitting at High Current Densities. Chemistry - A European Journal, 2017, 23, 10187-10194.	3.3	61
71	Highly stable three-dimensional nickel–iron oxyhydroxide catalysts for oxygen evolution reaction at high current densities. Electrochimica Acta, 2017, 245, 770-779.	5.2	37
72	Bimetallic Ni–Mo nitride nanotubes as highly active and stable bifunctional electrocatalysts for full water splitting. Journal of Materials Chemistry A, 2017, 5, 13648-13658.	10.3	191

#	Article	IF	CITATIONS
73	Structural formation and charge storage mechanisms for intercalated two-dimensional carbides MXenes. Physical Chemistry Chemical Physics, 2017, 19, 9509-9518.	2.8	19
74	Performance evaluation of asymmetric supercapacitor based on Ti3C2Tx-paper. Journal of Alloys and Compounds, 2017, 729, 1165-1171.	5.5	26
75	Crystal Co _{<i>x</i>} B (<i>x</i> = 1–3) Synthesized by a Ball-Milling Method as High-Performance Electrocatalysts for the Oxygen Evolution Reaction. ACS Sustainable Chemistry and Engineering, 2017, 5, 10266-10274.	6.7	76
76	New Ti 3 C 2 aerogel as promising negative electrode materials for asymmetric supercapacitors. Journal of Power Sources, 2017, 364, 234-241.	7.8	205
77	N-Doped graphene-supported Co@CoO core–shell nanoparticles as high-performance bifunctional electrocatalysts for overall water splitting. Journal of Materials Chemistry A, 2016, 4, 12046-12053.	10.3	91
78	Hollow CoP nanopaticle/N-doped graphene hybrids as highly active and stable bifunctional catalysts for full water splitting. Nanoscale, 2016, 8, 10902-10907.	5.6	158
79	A bismuth oxide nanosheet-coated electrospun carbon nanofiber film: a free-standing negative electrode for flexible asymmetric supercapacitors. Journal of Materials Chemistry A, 2016, 4, 16635-16644.	10.3	124
80	Hierarchical nickel–cobalt phosphide yolk–shell spheres as highly active and stable bifunctional electrocatalysts for overall water splitting. Nanoscale, 2016, 8, 19129-19138.	5.6	140
81	Electrochemically activated-iron oxide nanosheet arrays on carbon fiber cloth as a three-dimensional self-supported electrode for efficient water oxidation. Journal of Materials Chemistry A, 2016, 4, 6048-6055.	10.3	66
82	Coupling Hollow Fe ₃ O ₄ –Fe Nanoparticles with Graphene Sheets for High-Performance Electromagnetic Wave Absorbing Material. ACS Applied Materials & Interfaces, 2016, 8, 3730-3735.	8.0	427
83	Nanostructured molybdenum phosphide/N,P dual-doped carbon nanotube composite as electrocatalysts for hydrogen evolution. RSC Advances, 2016, 6, 7370-7377.	3.6	30
84	Two-dimensional titanium carbide electrode with large mass loading for supercapacitor. Journal of Power Sources, 2015, 294, 354-359.	7.8	199
85	Ultrathin MoSe ₂ Nanosheets Decorated on Carbon Fiber Cloth as Binder-Free and High-Performance Electrocatalyst for Hydrogen Evolution. ACS Applied Materials & Interfaces, 2015, 7, 14170-14175.	8.0	165
86	Facile fabrication of ZnO:S/ZnO hetero-nanostructures and their electronic structure investigation by electron energy loss spectroscopy. CrystEngComm, 2015, 17, 2250-2254.	2.6	4
87	Hierarchical nanosheet-based CoMoO ₄ –NiMoO ₄ nanotubes for applications in asymmetric supercapacitors and the oxygen evolution reaction. Journal of Materials Chemistry A, 2015, 3, 22750-22758.	10.3	140
88	Quantitative investigation on the effect of hydrogenation on the performance of MnO2/H-TiO2 composite electrodes for supercapacitors. Journal of Materials Chemistry A, 2015, 3, 3785-3793.	10.3	36
89	Controllable growth of ZnO–ZnSe heterostructures for visible-light photocatalysis. CrystEngComm, 2014, 16, 1201-1206.	2.6	46
90	Rationally designed hierarchical ZnCo ₂ O ₄ /Ni(OH) ₂ nanostructures for high-performance pseudocapacitor electrodes. Journal of Materials Chemistry A, 2014, 2, 20462-20469.	10.3	67

#	Article	IF	CITATIONS
91	Recognition of the Source Rock Using Biomarkers From Eocene Reservoir Oils. Petroleum Science and Technology, 2013, 31, 1689-1696.	1.5	1
92	Synthesis and transport properties of Si-doped In2O3(ZnO)3 superlattice nanobelts. CrystEngComm, 2011, 13, 3569.	2.6	10
93	Enhancement of near-band edge emission of Au/ZnO composite nanobelts by surface plasmon resonance. CrystEngComm, 2011, 13, 3678.	2.6	32
94	High-yield synthesis of In2â^'xGaxO3(ZnO)3 nanobelts with a planar superlattice structure. CrystEngComm, 2010, 12, 2047.	2.6	19